Supersymmetry Prospects at an Upgraded Fermilab Tevatron Collider

S. Mrenna
Argonne National Laboratory, Argonne, Illinois 60439
M. Diwan
Brookhaven National Laboratory, Upton, New York 11973
S. Lammel
Fermi National Accelerator Laboratory, Batavia, Illinois 60510
H. Baer
Florida State University, Tallahassee, Florida 32306
M. Barnett, A. Barbaro-Galtieri, W.-M. Yao
Lawrence Berkeley National Laboratory, Berkeley, California 94720
K. De, M. Sosebee
University of Texas at Arlington, Arlington, Texas 76019
T. Kamon, D. Norman, J.T. White
Texas A&M University, College Station, Texas 77843

ABSTRACT

The Fermilab Tevatron is currently the highest energy collider in the world. For the next ten years, while the Large Hadron Collider is being constructed at CERN, the Tevatron will remain the premier machine to search for new physics like supersymmetry. Moderate upgrades to the machine and experiments will enable physicists to explore many interesting regions in supersymmetric parameter space. The TeV33 upgrade project at the Tevatron is planned for the beginning of the next decade. In this paper we show the potential of the TeV33 project to discover supersymmetry, to distinguish between different models and to measure the first supersymmetric parameters.

I. OVERVIEW

The Standard Model (SM) of particle physics is in remarkably good agreement with existing data. In spite of this fact, there are strong theoretical arguments to suggest that the SM will break down in the TeV domain. Thus, high energy physics is currently in the position of having a theory that works at a level of high precision, but must in fact be modified at an energy scale not far above the energy of existing accelerators. The Large Hadron Collider (LHC) would provide access to new physics at the TeV-scale when it becomes operational in about ten years. In the meantime, modest upgrades to the Tevatron could provide important evidence for new physics and help map out the strategy for further explorations at the LHC and the proposed Next Linear Collider (NLC).

Any model of new physics must face the difficult task of accommodating the high precision tests of the SM, and yet significantly modifying it at an energy scale not much beyond that of the Z boson. Supersymmetry[1] (SUSY) provides such a framework because of the rapid decoupling of SUSY partners from SM particles. In addition, the solution that supersymmetry gives to the hierarchy problem requires that there be a large number of new SUSY particles lying approximately between 100 GeV/c^2 and 1 TeV/c^2. Experimental searches for the SUSY particles have examined only a very small part of this expected mass range, so it is not surprising that the SUSY particles have not yet been discovered. It is thus of importance for new accelerators to try to increase the mass reach if supersymmetry is to be tested.

Extensive work was done during the TeV2000 studies[2] to delineate the discovery reach of various Tevatron upgrades in supersymmetric parameter space. Much effort was also devoted to understanding the degradation of discovery reach in a high luminosity environment. It is possible that the first signals for supersymmetry (or deviations from the Standard Model) will be observed at LEP2 or in Run II of the Tevatron. At Snowmass, we chose several points in supersymmetric parameter space assumed to be discoverable by Tevatron Run II. Our goal was to try to ascertain the capability of an upgraded Tevatron to perform precision measurements of supersymmetric particles, and to measure fundamental parameters. We show in this report that the large increase in luminosity may allow not only for the discovery of supersymmetry, but also may give sufficiently significant event rates that several precision measurements of underlying parameters will be possible.

II. MINIMAL SUPERGRAVITY MODEL

For the studies performed in this report, we adopt the theoretical framework of the minimal supergravity model (mSUGRA), which is described in greater detail in the Report of the Supersymmetry Theory Subgroup[1]. Briefly, this model adopts the particle content and interactions of the Minimal Supersymmetric Standard Model (MSSM), but with additional assumptions due to theoretical prejudice about physics at the grand unification (GUT) scale. It assumes the MSSM is a valid theory at energies ranging from the weak scale to the GUT scale. Inspired by the simplest supergravity GUT models, it assumes

a common GUT scale scalar mass m_0, a common GUT scale gaugino mass $m_{1/2}$ and a common GUT scale trilinear coupling A_0. The various couplings and soft-SUSY breaking terms are evolved from the GUT scale down to the weak scale via renormalization group equations. Electroweak symmetry is broken radiatively owing to the large top Yukawa coupling, which allows determination of the magnitude (but not the sign) of the Higgsino mixing parameter μ in terms of M_Z, and allows elimination of the bilinear soft term B in lieu of $\tan\beta$, the ratio of Higgs field vaccum expectation values. Thus, the parameter set ($m_0,\ m_{1/2},\ A_0,\ \tan\beta$ and $sgn(\mu)$) completely determines all SUSY particle masses and mixings. Note that this framework assumes only an $SU(3)\times SU(2)\times U(1)$ gauge structure, and so does not include effects from any particular GUT group choice.

Several experimental successes have led to the acceptance of the model described above. It provided a simple mechanism for grand unification of the precision LEP measurements. Further, unification occurs if SUSY masses are precisely in the range needed to resolve the gauge hierarchy problem. The model is also consistent with low energy SM tests. If, in addition, the $SU(5)$ GUT group is hypothesized, the model is still allowed by current bounds on proton decay. Finally, the condition of R-parity invariance leads to a stable lightest supersymmetric particle (LSP) which provides the right amount of dark matter over a large fraction of the supersymmetric parameter space[3]. This agreement is non-trivial as the relic dark matter density depends on such disparate quantities as the electroweak coupling constant, the LSP mass, the gravitational constant and the Hubble constant.

If one adds additional light Higgs doublets to the particle spectrum, agreement with grand unification (or proton decay bounds in the case of $SU(5)$) is lost, while a Higgs singlet would generally destabilize the gauge hierarchy. While the assumption of exactly four generations is still consistent with grand unification, it would ruin the prediction of m_b/m_τ for groups such as $SU(5)$ or $SO(10)$. Thus, the chosen model is fairly constrained, and it is therefore reasonable to use it as the prototype for testing accelerator capabilities.

A model with so few parameters allows a number of predictions of the mass spectrum. Thus, there are a number of light particles present, *e.g.*, the light Higgs (h) has a mass bound $m_h \lesssim 130$ GeV/c^2 ($m_h \lesssim 150$ GeV/c^2 for a theory with arbitrary Higgs content). The theory also predicts the existence of a light chargino ($\chi_1^\pm$) and two light neutralinos ($\chi_{1,2}^0$). For example, for $\mu^2 \gg M_Z^2$ (*i.e.*, $\mu \gtrsim 3M_Z$) one has $m_{\chi_1^\pm} \simeq m_{\chi_2^0} \simeq 2\ m_{\chi_1^0} \simeq (\frac{1}{3}\sim\frac{1}{4})m_{\tilde{g}}$. The χ_1^0 is the LSP for almost the entire parameter space.

The spectrum of supersymmetric particles in mSUGRA is shown in Table I. Note that $\tilde{t}_i, \tilde{b}_i$, and $\tilde{\tau}_i$ ($i = 1, 2$) are mixtures of the corresponding left- and right- chiral scalar fields, charginos are mixtures of charged higgsino and wino, and neutralinos are mixtures of two neutral higgsinos, bino and the neutral wino.

At hadron colliders, sparticles can be produced via the following lowest-order reactions:

- $q\bar{q},\ gg,\ qg\to\widetilde{g}\widetilde{g},\ \widetilde{g}\widetilde{q},\ \widetilde{q}\widetilde{q}$ (strong production)

Table I: List of supersymmetric partners and Higgs bosons.

Particle Name	Spin	Physical States
squarks	0	$\tilde{d}_L, \tilde{u}_L, \tilde{s}_L, \tilde{c}_L, \tilde{b}_1, \tilde{t}_1,$ $\tilde{d}_R, \tilde{u}_R, \tilde{s}_R, \tilde{c}_R, \tilde{b}_2, \tilde{t}_2$
sleptons	0	$\tilde{e}_L, \tilde{\nu}_{eL}, \tilde{\mu}_L, \tilde{\nu}_{\mu L},$ $\tilde{\tau}_1, \tilde{\nu}_{\tau L}, \tilde{e}_R, \tilde{\mu}_R, \tilde{\tau}_2$
charginos	$\frac{1}{2}$	$\chi_1^\pm, \chi_2^\pm$
neutralinos	$\frac{1}{2}$	$\chi_1^0, \chi_2^0, \chi_3^0, \chi_4^0$
gluino	$\frac{1}{2}$	$\widetilde{g}$
Higgs bosons	0	h, H, A, $H^\pm$

- $q\bar{q},\ qg\to\widetilde{g}\chi_i^0,\ \widetilde{g}\chi_i^\pm,\ \widetilde{q}\chi_i^0,\ \widetilde{q}\chi_i^\pm$ (associated production)
- $q\bar{q}\to\chi_i^\pm\chi_j^\mp,\ \chi_i^\pm\chi_j^0,\ \chi_i^0\chi_j^0$ (χ pair production)
- $q\bar{q}\to\widetilde{\ell}\widetilde{\nu},\ \widetilde{\ell}\widetilde{\ell},\ \widetilde{\nu}\widetilde{\nu}$ (slepton pair production)

Once produced, sparticles rapidly decay to other sparticles initiating a cascade which ends with the LSP (χ_1^0).

III. CURRENT STATUS OF THE SEARCH FOR SUSY

The current mass limits on supersymmetric particles and the light Higgs particle are shown in Table II. Most of the current lower limits are below or near the low end of the expected SUSY mass spectrum. It is is not surprising that they have not been discovered. However, naturalness arguments suggest that some of the SUSY masses may be quite close to these lower limits[4]. TeV33 may provide one of the first opportunities to explore a substantial fraction of the expected SUSY spectrum. Note that some of these limits depend on the choice of a spe-

Table II: Current mass limits on supersymmetric partners and light Higgs. Some limits are model dependent – lower mass particles possible under certain circumstances.

Particle	Mass Limit	Comments
$\widetilde{g}$	173 GeV/c^2	DØ & CDF
$\widetilde{q}$	229 GeV/c^2	DØ & CDF ($M_{\widetilde{q}} = M_{\widetilde{g}}$)
$\widetilde{t}_1$	100 GeV/c^2	DØ ($\widetilde{t}_1 \to c\chi_1^0$)
$\widetilde{t}_2$	48 GeV/c^2	LEP140 ($M_{\chi_1^0}$ = 30 GeV/c^2)
$\chi_1^\pm$	65 GeV/c^2	LEP140 ($M_{\chi_1^\pm} - M_{\chi_1^0} > 10$ GeV/c^2)
$\chi^0{}_2$	69 GeV/c^2	LEP140 ($M_{\chi_2^0} - M_{\chi_1^0} > 10$ GeV/c^2)
χ_1^0	20 GeV/c^2	LEP
$\widetilde{\ell}$	45 GeV/c^2	LEP
$\tilde{e}$	53 GeV/c^2	LEP140 ($M_{\chi_1^0} < 35$ GeV/c^2)
$\widetilde{\nu}$	43 GeV/c^2	LEP
h	60 GeV/c^2	LEP

cific supersymmetric model. Lower mass particles may exist depending on the choice of SUSY parameters.

As an example, we illustrate a slice of the m_0 vs. $m_{1/2}$ mSUGRA parameter space in Fig. 1, for $\tan\beta = 2$, $\mu > 0$ and $A_0 = 0$. The bricked regions are excluded by theoretical constraints (improper Electro-Weak symmetry breaking or a charged LSP), while the shaded regions are excluded by the mass bounds from Table II. Contours of constant $m_{\tilde{g}}$, $m_{\tilde{q}}$ and $m_{\chi_1^\pm}$ are shown as well.

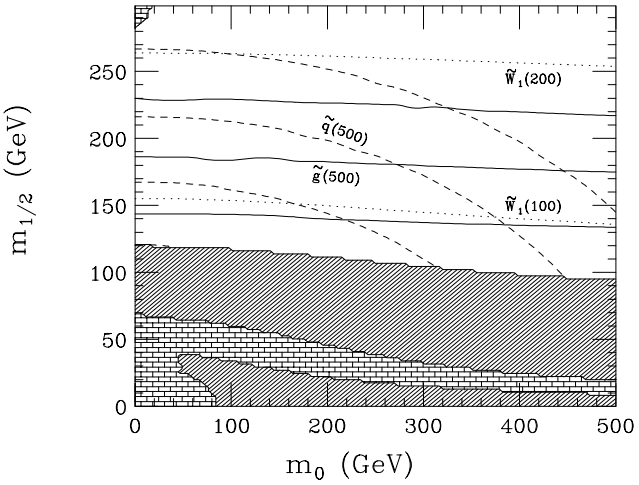

Figure 1: Contours of gluino, squark and chargino mass in the m_0 vs. $m_{1/2}$ plane for $\tan\beta = 2$, $A_0 = 0$ and $\mu > 0$.

IV. DISCOVERY REACH OF TEV33

Production and decay of SUSY particles at the Tevatron collider can lead to many different signatures which may yield evidence for supersymmetry[5]. In particular, in many regions of parameter space, a signal for SUSY could be found above SM background rates by looking for *i*) multi-jet +$\not\!\!E_T$ events (no isolated leptons), *ii*) single isolated lepton + multi-jets +$\not\!\!E_T$ events, *iii*) isolated dilepton + multi-jets +$\not\!\!E_T$ events (opposite sign (OS) or same-sign (SS)), *iv*) isolated trilepton + multi-jets +$\not\!\!E_T$ events, *v*) clean (jet-free) isolated trilepton +$\not\!\!E_T$ events, and *vi*) clean (jet-free) isolated dilepton +$\not\!\!E_T$ events. In addition, other channels are possible, and are generally less promising.

Of the above channels, the clean trilepton channel is generally regarded as most promising, since it allows SUSY to be discovered at a high luminosity Tevatron collider over the largest region of parameter space[6]. We show in Fig. 2 the same m_0 vs. $m_{1/2}$ plane as in Fig. 1[7]. The grey boxes are parameter space points where the Tevatron Main Injector (2 fb^{-1} of integrated luminosity) should be able to discover supersymmetry, while the white boxes are points where TeV33 should be able to discover supersymmetry. Note the maximum reach in $m_{1/2}$ corresponds to a gluino mass of over 700 GeV/c^2! There also exist regions (large m_0 and low $m_{1/2}$ where interference effects in the neutralino leptonic branching fraction lead to no reach at all.

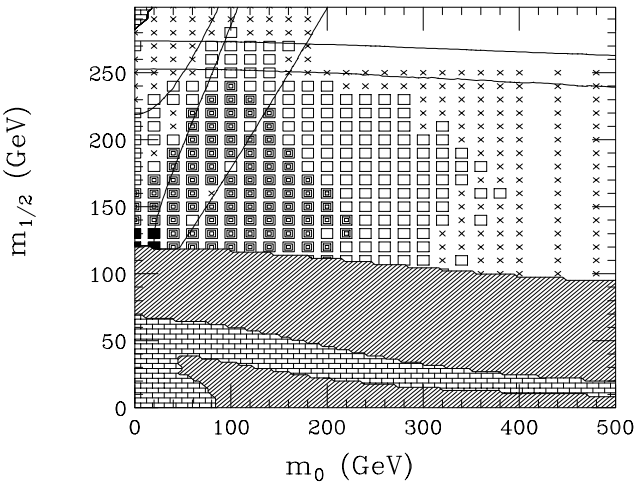

Figure 2: Parameter space reach of Tevatron Main Injector (grey boxes) and TeV33 (white boxes) for the same parameter plane as in Fig. 1, via the clean trilepton channel.

Such a plot can also be made as a function of the chargino mass. Figure 3 is taken from Ref.[8], and illustrates the model dependence of the chargino mass accessible via the clean trilepton search. The cross section times branching fraction times detection efficiency is plotted as a function of the $\chi_1^\pm$ mass. Typical DØ and CDF detection efficiencies have been applied. Each point in the plot represents the prediction from a specific

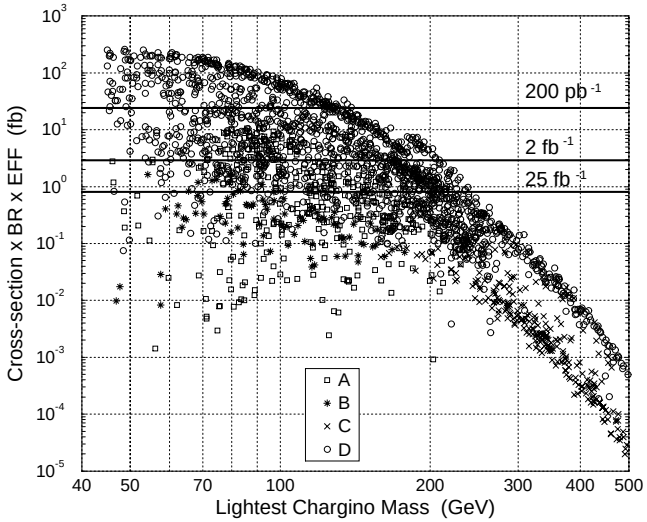

Figure 3: Total supersymmetric trilepton signal ($\sigma \times BR \times$EFF) versus the lightest chargino mass[8]. The branching ratio (BR) is defined as the fraction of $\chi_1^\pm \chi_2^0$ events that decay to 3 leptons. The efficiency (EFF) is the fraction of 3 lepton events that pass the cuts. The 5σ significances for integrated luminosities 200 pb^{-1}, 2 fb^{-1}, and 25 fb^{-1} are shown by the dark horizontal lines. The different symbols correspond to when the χ_2^0 has (A) a neutral "invisible" branching ratio $> 90\%$, (B) a large destructive interference in 3-body leptonic decays, (C) a branching ratio to Higgs $> 50\%$, or (D) all other solutions.

Table III: Summary of SUSY mass reaches obtainable at various colliders. "Exhaustive Reach" means the mass limit for any choice of parameters. Searches at LHC are not shown here.

Collider	LEP2	TeV33		NLC
$\sqrt{s}$	190 GeV	2 TeV		500 GeV
$\int \mathcal{L}dt$	500 pb^{-1}	25 fb^{-1}		20 fb^{-1}
	Max. reach	Exhaustive reach	Max. reach	Max. reach
$\chi_1^\pm$	90 GeV/c^2	N/A	250 GeV/c^2	248 GeV/c^2
$\tilde{g}/\tilde{q}$	85 GeV/c^2 (100 pb^{-1})	275 GeV/c^2	$>$ 450 GeV/c^2	$\sim$250 GeV/c^2
$\tilde{t}_1$ ($\rightarrow c\chi_1^0$)	83 GeV/c^2	45 GeV/c^2 (2 fb^{-1})	120 GeV/c^2 (2 fb^{-1})	$\sim$250 GeV/c^2
$\tilde{t}_1$ ($\rightarrow b\chi_1^\pm$)	N/A	150 GeV/c^2	180 GeV/c^2	$\sim$250 GeV/c^2

mSUGRA parameter space point. We find that the minimum $\sigma \cdot BR \cdot \epsilon_{tot}$ for integrated luminosities of 2 fb^{-1} and 10 fb^{-1} are 3.0 fb and 1.3 fb respectively, by requiring the number of signal events which yield a 5σ significance above background. The maximum $\chi_1^\pm$ masses we can probe are 210 GeV/c^2 and 235 GeV/c^2. Note that for a few models, $\chi_1^\pm$ might escape detection with much lower masses.

The mass reach from *all* discovery channels can be combined on a single plot. This is done in Fig. 4, for the same frame as Fig. 1. The black squares denote points accessible by the current Tevatron experiments (0.1 fb^{-1}). Comparing Fig. 4 to Fig. 2, it is easy to see that most of this reach is achieved via the clean trilepton searches.

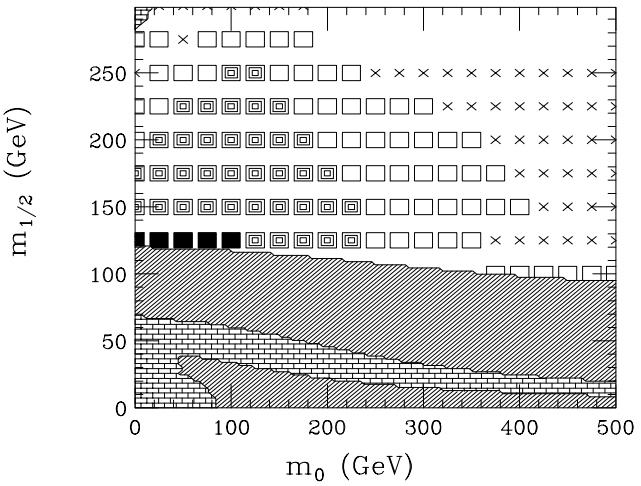

Figure 4: Parameter space reach of Tevatron Main Injector (grey boxes) and TeV33 (white boxes) for the same parameter plane as in Fig. 1, where *all* channels are included.

The SUSY mass reach at TeV33 (25 fb^{-1}) is compared to the reach expected at LEP2 and the NLC in Table IV. While LEP2 can find or exclude the light chargino ($\chi_1^\pm$) and light top-squark ($\tilde{t}_1$) masses up to nearly its kinematical limit ($\sqrt{s}/2$), searches at TeV33 could obtain a maximum reach 2-3 times that of LEP2. If LEP2 found a 90 GeV/c^2 chargino, we would expect a 270-360 GeV/c^2 gluino at TeV33 for the mSUGRA model. Such a gluino should be easily detectable at TeV33. It should also be possible to gain a rough measure of the gluino mass at TeV33. TeV33 is also competitive to the NLC in the gluino/squark searches. Thus, the SUSY searches at TeV33 are complementary to those at LEP2[9] and the NLC.

V. MEASUREMENT OF SUSY PARAMETERS

In consultation with the SUSY Theory Subgroup, we have chosen four points for detailed studies at Snowmass (see Table IV). These points do not exhaust all possible supersymmetric signatures at the Tevatron. Rather, they exemplify a few of the many signatures that may be accessible at the Tevatron – signatures which are crucial in order to show that supergravity-inspired low energy supersymmetry is (or is not) the underlying theory behind any observed deviation from the Standard Model.

Table IV: SUSY parameter points studied at Snowmass. Point 2 is the Common Point.

	m_0	$m_{1/2}$	A_0	$\tan\beta$	sgn(μ)
	All masses in GeV/c^2				
Point 1	100	150	0	2	-1
Point 2	200	100	0	2	-1
Point 3	200	125	0	10	-1
Point 4	200	130	-400	2	$+1$

	$m_{\tilde{g}}$	$m_{\tilde{q}}$	$m_{\chi_1^\pm}$	$m_{\tilde{t}_1}$	$m_{\chi_1^0}$
	All masses in GeV/c^2				
Point 1	413	372	135	315	65
Point 2	298	317	96	264	45
Point 3	369	368	92	269	50
Point 4	371	373	88	140	46

Our Point 2 was chosen to be the same as NLC Point 3 and LHC parameter space Point 4, and will be referred to as the Common Point. The top quark mass was set to 175 GeV/c^2 in the simulations. Note that all points chosen yield reasonable values for the cosmological neutralino dark matter relic density[3].

A. Event generation and simulation

We have used ISAJET[10] v7.13/v7.20 to generate all the final states for the chosen points, and used v7.20 for the background events. We have used a detector simulation package provided by F. Paige[11]. The following resolutions were used to model the calorimeters for a TeV33 detector:

EM Cal	$15\%/\sqrt{E}\oplus 2\%$
Hadronic Cal	$50\%/\sqrt{E}\oplus 3\%$
Forward Cal	$80\%/\sqrt{E}\oplus 3\%$ for $\|\eta\| > 3.4$.

Jets were found using a simple fixed-cone algorithm with $R = 0.7$ in the region $|\eta| < 3.4$ and $E_T > 8$ GeV.

B. The Supersymmetric Trilepton Signature

The trilepton signature has great potential for being the discovery channel for SUSY. There are very few Standard Model backgrounds, primarily W and Z boson pair production with each boson decaying leptonically. The SUSY trilepton signature results from the associated production of $\chi_1^\pm \chi_2^\circ$ fermion pairs. It has been shown that the discovery reach for TeV33 is significant for the trilepton signature. If SUSY is discovered, and the production of SUSY particles produces a significant trilepton signature, one would like to measure the underlying physics of SUSY - the various parameters defining the theory. This section deals with what might be possible to learn about SUSY given a sample of trilepton SUSY events.

The primary focus of this study is to distinguish various points in mSUGRA parameter space using the trilepton signature. In this section, we compare the clean trilepton signal from Point 1 (P1) and the Common Point (P2).

1. Trilepton Event Selection and Backgrounds

For the next collider run of the Tevatron with the Main Injector, the expected integrated luminosity for each of the two collider experiments is 2 fb^{-1}. For TeV33 the current working scenario is 30 fb^{-1}. One question to answer is how many signal events do we expect to see for the two points. For 30 fb^{-1} we expect 500 events for the Common Point and 425 events for Point 1 using the cuts shown in the next paragraph. From background samples of WZ boson pairs and top quark production we find that we should expect to see 190 WZ boson pairs and 75 top events. These numbers are determined by generating Monte Carlo samples using ISAJET v7.13.

Trilepton events are selected by requiring one lepton (muon or electron) with p_T greater than 15 GeV/c and two additional leptons with p_T greater than 10 GeV/c. We require that the missing E_T be greater than 20 GeV. Since both SUSY particles produced in these events decay leptonically, we require that the events be relatively quiet hadronically by requiring that there be no more than one jet in the event. This jet cut is applied primarily to separate the direct production of $\chi_1^\pm \chi_2^\circ$ pairs from squark and gluino production which can produce charginos and neutralinos in their cascade decays along with a large number of jets, and to reduce $t\bar{t}$ background. We estimate a combined trigger, tracking, and lepton identification efficiency of 47% from our experience with the latest Tevatron collider data. The total branching fraction to three leptons times kinematic efficiency is 4.6% for Point 1 where the production cross section is 0.65 pb. For the Common Point with a production cross section of 3.24 pb, the total branching fraction to three leptons times kinematic efficiency is 1.08% .

In Fig. 5, we plot the invariant mass of the two leptons which are most likely to come from the Z boson or χ_2° (opposite charge, same species, and closest in proximity) for the Common Point (solid line) and WZ boson pair (dashed line) Monte Carlo samples. As one can see the Common Point distribution

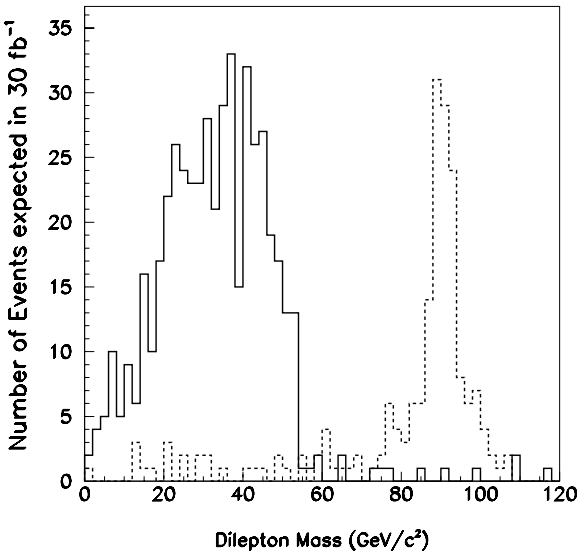

Figure 5: The dilepton mass distributions of the Common Point (solid) and WZ boson pair (dashed) Monte Carlo samples.

is quite distinct from the WZ boson pair background, which can be removed by a mass cut. The mass difference for the χ_2° (mass = 97.3 GeV/c^2) and χ_1° (mass = 44.6 GeV/c^2) is given by the upper edge of the Common Point distribution[12]. The top background mass distribution (not shown) is flat and is about at the same level on the plot as the tails of the WZ boson pair distribution. From this simulation of Common Point signal and background, it is apparent that the mass difference of the two lightest neutralinos can be measured.

2. Differentiating between SUSY Models

In the case of the Common Point, the χ_2° is lighter than the sleptons – thus it can decay into a χ_1° and a pair of same-flavor leptons through a virtual Z boson. The maximum value for the invariant mass of the lepton pair occurs when the χ_1° particle is at rest in the three body decay. Therefore, this maximum value corresponds to the mass difference between the two neutralinos. This technique provides a powerful method for constraining the neutralino mass spectrum.

In the case of Point 1, the charged sleptons are lighter than the χ_2° fermion, such that the χ_2° decays to a real charged right handed slepton and a lepton with a branching fraction of about 85%. The slepton then decays to lepton and χ_1°. Since this is

a cascade of two body decays, the endpoint of the two-lepton mass need not be the mass difference of the two neutralinos. Therefore, we cannot determine the neutralino mass difference for this point. In addition, it would not even be possible to distinguish between the two models described by Points 1 and 2 based on the mass difference.

In Fig. 6 are shown four frames of distributions in different variables. The solid line is Point 1 and the dashed line is the Common Point. The plots have been normalized to the number of events in each sample. Plot A is the dilepton mass (Var1). As

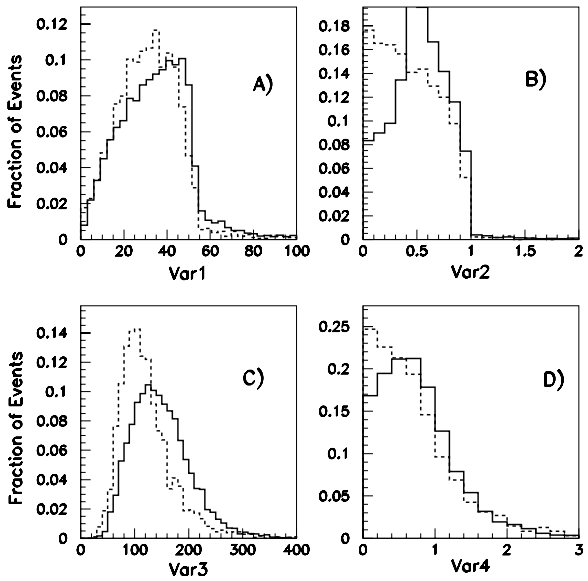

Figure 6: Various distributions for Point 1 (solid) and the Common Point (dashed) showing the similarities and differences for these two models. The histograms have been normalized to the number of events and are described in detail in the text.

one can see the upper edge of the distribution for both points is about 55 GeV/c^2, consistent with the mass difference of the two lightest neutralinos for the Common Point. However, for Point 1, the masses of the two lightest neutralinos are 135.5 and 65.3 GeV/c^2 respectively with a difference of about 70 GeV/c^2.

What might be done to distinguish these two scenarios? The different paths of the decay of the χ_2° for the two points do lead to different kinematic signatures. This is shown in plots B and D of Fig. 6. In plot B (Var2), the scalar difference in the p_T of the two leptons from the χ_2° (as defined above) divided by the magnitude of the sum of the momentum vectors of the two leptons, is histogrammed. For the case where the χ_2° decays via sleptons, one expects the p_T of the two leptons to be more unequal compared to the case where the χ_2° decays via three-body decay modes. In plot D (Var4), the difference in the missing E_T and the p_T of the third leading lepton, divided by the scalar sum of the p_T of the two leading leptons, is given. Plot C gives the scalar sum (Var3) of the p_T of the three leading leptons and the missing E_T. The difference in the two distributions in plot C reflects the fact that the masses of the SUSY gauginos in the Point 1 scenario are heavier than those of the Common Point.

3. Maximum Likelihood Fit to the Trilepton Signal

There may be other similar distributions like those in Fig. 6, and given 400–500 events it may not to be too difficult to match the data to the best model (or at least class of models). But in Run II of the Tevatron collider with Main Injector, we expect only 20-30 events from scenarios like Point 1 or the Common Point. For so few events, it may be possible to use fitting procedures such as neural networks to at least constrain potential models (*e.g.* fits may indicate a model that has light sleptons). To test this a simple log likelihood calculation was used to try to distinguish the two mSUGRA scenarios. The distributions B), C), and D) in Fig. 6 were used to calculate the log likelihood value for samples of Point 1 and Common Point Monte Carlo. We calculate a log likelihood discriminant, which is the difference in the log likelihood calculated from the Point 1 and Common Point distributions. If $LL2$ is the value of the log likelihood calculated from the Common Point distributions and $LL1$ from Point 1, then the discriminant ($LL2 - LL1$) is on average negative for events from the Point 1 model and positive for events from the Common Point model. Thus, an ensemble of events could be classified as more likely to be from Point 1 rather than the Common Point. By selecting an appropriate set of distributions that define the unique difference between two models or class of models, it may be possible to determine that a set of events excludes one model or class of models.

Assuming that we have 20 events from one or the other of the two models (expected from the Tevatron's Run II), we calculate the value of the discriminant and calculate the average. We do this for many sets of twenty events for both Point 1 and the Common Point. The average is plotted in Fig. 7. P1 is Point 1 and P2 is the Common Point. The distributions were normalized by the number of sets of 20 events, so the histogram represents the probability of getting the indicated values of the

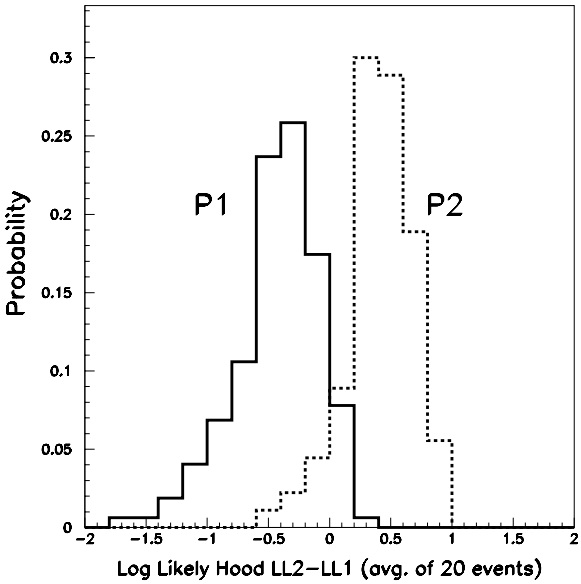

Figure 7: The average value of the discriminant $LL2 - LL1$ for many ensembles of 20 events for the Common Point (P2) and Point 1 (P1).

discriminant for P1 and P2 averaging over 20 events. If a cut of 0 on $LL2 - LL1$ was used to distinguish between P1 and P2, then there is a 9% chance that if P1 is the true model (or class of model), we could make the incorrect choice. Similarly, there is a 7% chance that if P2 is the true model, we would make the incorrect choice with a cut at 0. With higher statistics, the probability of ascertaining the correct model increases. Though the above study was done for a Run II scenario, similar techniques may be used for low statistics SUSY signals at TeV33.

C. The $b\tilde{b}$ Signature from Gluino Decays

We report here results for Point 2, which is the common comparison point. The cross section for gluino production is quite large at the Tevatron for this point. The branching ratios into bottom quarks are also very large.

The cross section for the processes involving gluino production is:

$$\sigma(p\bar{p} \rightarrow \tilde{g} + X) = 0.783\, pb.$$

The masses of the SUSY Particles involved in the gluino production and decay are as follows:

$$M_{\tilde{g}} = 298 \text{ GeV/c}^2$$
$$M_{\tilde{b}} = 278 \text{ GeV/c}^2$$
$$M_{\chi_2^0} = 98 \text{ GeV/c}^2$$
$$M_{\chi_1^0} = 44 \text{ GeV/c}^2$$

The branching ratios relevant to our study are as follows:

$$\tilde{g} \rightarrow \tilde{b}b = \quad 88.6\%$$
$$\tilde{b} \rightarrow \chi_2^0 b = \quad 86.3\%$$
$$\chi_2^0 \rightarrow \chi_1^0 \ell^+\ell^- = \quad 33.2\ \% \quad \text{with } \ell = e, \mu$$

The cascade decay sequence of the gluino that we studied is then:

$$\tilde{g} \rightarrow \tilde{b}b,\ \ \tilde{b} \rightarrow \chi_2^0 b,\ \ \chi_2^0 \rightarrow \chi_1^0 \ell^+\ell^-,$$

where χ_1^0 is the LSP. Thus, the gluino signature would be the presence of two opposite sign leptons (2 e's or 2 μ's if we neglect the τ pair decay mode), two bottom quarks and $\not\!\!E_T$.

It is expected that with the large cross section for $\tilde{g}$ and using an efficient b-tagging algorithm (which can be easily obtained with the planned silicon detectors for CDF and DØ in Run II and the CDF experience in Run I), we can obtain a healthy signal in Run II at TeV33 with 30 fb^{-1} of data. The major background to this signal would be $t\bar{t}$ production, which has a cross section $\sigma \sim 6.8$ pb.

Can we measure any of the SUSY particle masses with this final state? A method for measuring the $\tilde{g}$ and the $\tilde{b}$ mass, once the masses of χ_2^0 and χ_1^0 are known, was suggested at this Workshop by W.-M. Yao[13], who applied it first to LHC Monte Carlo events. We repeat that analysis here.

1. Event Selection and Mass Analysis

We reduce Standard Model and instrumental backgrounds with the following requirements:

- Electrons : $p_T > 8$ GeV/c, $|\eta| < 2.0$
- Muons : $p_T > 8$ GeV/c, $|\eta| < 1.4$
- Require at least two isolated leptons of the same flavor with opposite sign.
- b jets : $E_T > 10$ GeV, $|\eta| < 2.0$. A b-tagging efficiency of 66% is assumed.
- Require at least two identified b-jets.
- $\not\!\!E_T > 20$ GeV.

The same cuts were applied to the signal events and the top background events reported here.

Figure 8 shows the invariant mass of the two leptons for both signal and background. It shows a broad peak at about 35 GeV/c^2 with a sharp fall at about 45-50 GeV/c^2. The background from SUSY events, as well as from top quark events, exhibits a more flat behavior.

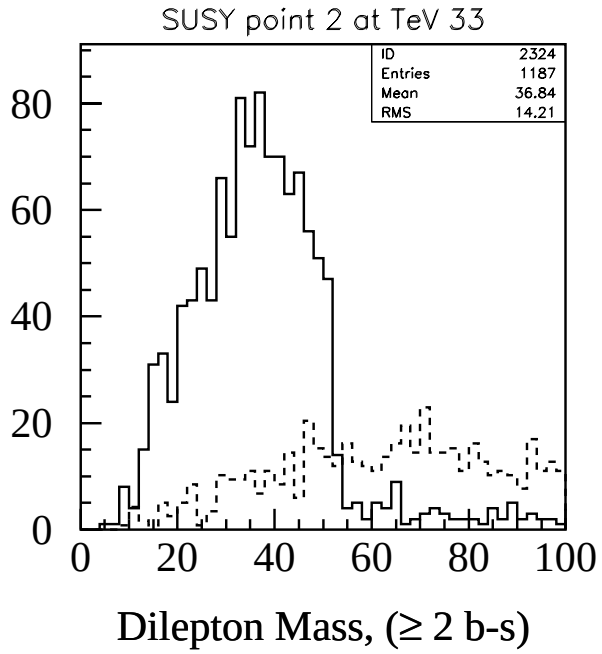

Figure 8: The dilepton invariant mass distribution from SUSY (solid line) and top production (dashed line), for 30 fb^{-1} of data at TeV33. Common point 2 is used. Events were required to contain at least 2 b-tags, as described in the text.

If we interpret this spectrum as due to the $\chi_2^0 \rightarrow \chi_1^0 \ell^+\ell^-$ decay, the sharp fall in the high part of the spectrum corresponds to the point in the Dalitz plot at which both the χ_1^0 and the $\ell^+\ell^-$ system are at rest. As pointed out in Ref [13] at this particular point the momentum of both the χ_1^0 and the χ_2^0 can be easily calculated in terms of the measured momentum of the $\ell^+\ell^-$ system and the χ_1^0 mass. The value at the edge of the spectrum

corresponds to the neutralino mass difference, which is approximately equal to the χ_1^0 mass since $m_{\chi_2^0} \sim 2 \times m_{\chi_1^0}$ for the SUSY models considered here.

Assuming that we know the mass of the χ_2^0, we can combine the χ_2^0 with any of the identified b jets to get the $\tilde{b}$ invariant mass distribution, then combine another of the b jets with $m_{\tilde{b}}$ to obtain the $\tilde{g}$ mass distribution. Figure 9 shows the mass difference $\Delta(m_{\tilde{g}} - m_{\tilde{b}})$ versus $m_{\tilde{b}}$.

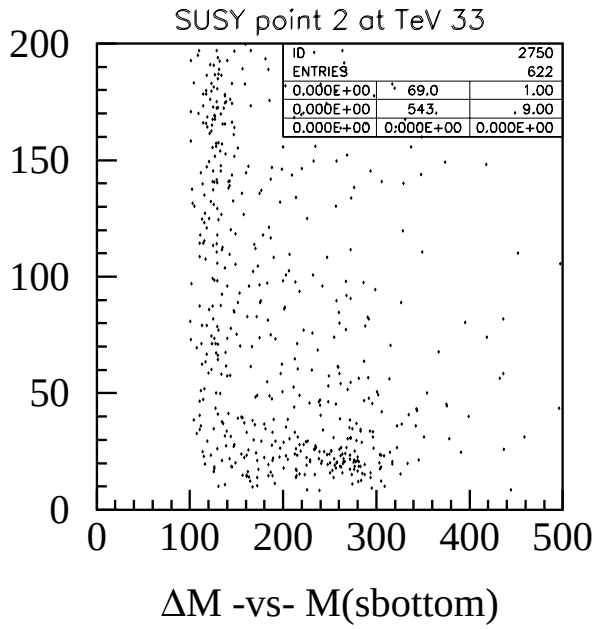

Figure 9: The gluino-sbottom mass difference versus the sbottom mass for 30 fb^{-1} of data at TeV33. Common point 2 is used.

We notice some concentrations of events, one at low Δm values, another at low $m_{\tilde{b}}$ values, and another at $m_{\tilde{b}}$ around 280 GeV/c^2. It is clear that the cluster at $m_{\tilde{b}}$ = 280 GeV/c^2 is correlated with the low Δm cluster and that by cutting at low Δm we reduce the background. This is a technique employed at both SPEAR and CLEO for charm and bottom particle mass measurements. Finally, Fig. 10 shows the projection on the Δm axis as well as the projection on the sbottom mass axis after a $\Delta m < 45$ GeV/c^2 cut.

The result of a fit to the Δm plot is 23.3 $\pm$ 1.2 GeV/c^2, very close to the expected value of 20 GeV/c^2. It is clear that there are sufficient events to measure the mass difference with reasonable precision. Also, the sbottom signal is sufficient for a good measurement. We have not done studies of the systematic errors associated with such measurements.

D. The Missing E_T plus Jets Signature

If the gluino or squarks are sufficiently light, the upgraded Tevatron should allow detection via the standard "missing E_T plus jets" signature. The missing E_T distributions from all SUSY sources in the Comparison Point are shown in Fig. 11. For missing E_T less than 100 GeV, the total distribution is dominated by chargino-neutralino combinations. Above 100 GeV,

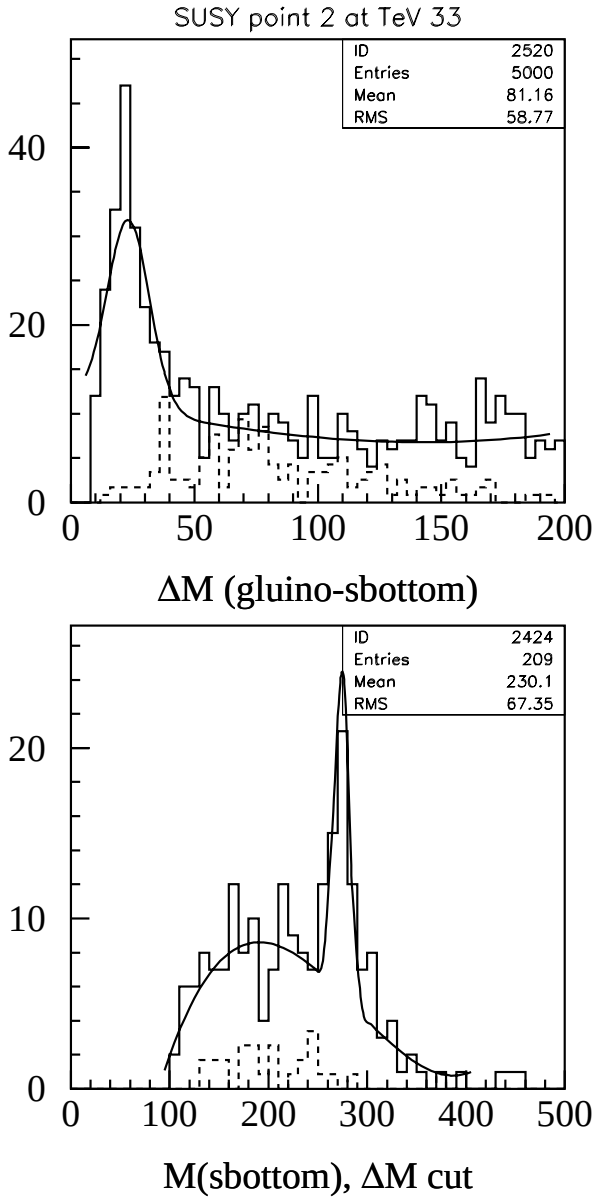

Figure 10: The gluino-sbottom mass difference, top, and the reconstructed sbottom mass from SUSY (solid line) and background top production (dashed line), for 30 fb^{-1} of data at TeV33. Common point 2 is used.

the distribution is dominated by gluino-squark and associative production combinations. The different contributions are labeled on the figure.

For this point, the gluino mass was 298 GeV/c^2 and the average squark mass was 317 GeV/c^2. To get an indication of how the SUSY signal compares to Standard Model backgrounds, a simple, non-optimized selection was made requiring ≥ 3 jets with $E_T > 30$ GeV, H_T (sum of all jet E_T's) > 200 GeV, and missing $E_T > 100$ GeV. The resulting distribution is shown in Fig. 12. The plot includes the distribution for the dominant background, $Z \rightarrow \nu\bar{\nu}$ + jets. Additional backgrounds from mismeasured W and Z events and top production will likely increase the background by a factor of at least two.

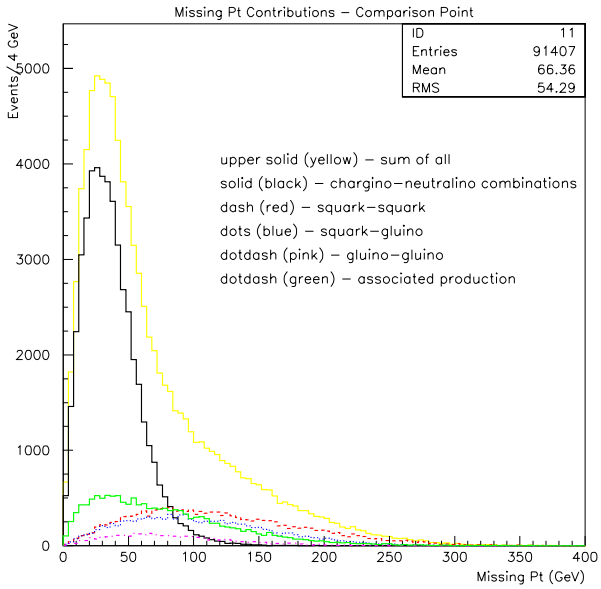

Figure 11: Missing E_T distribution from all SUSY sources for the Comparison Point.

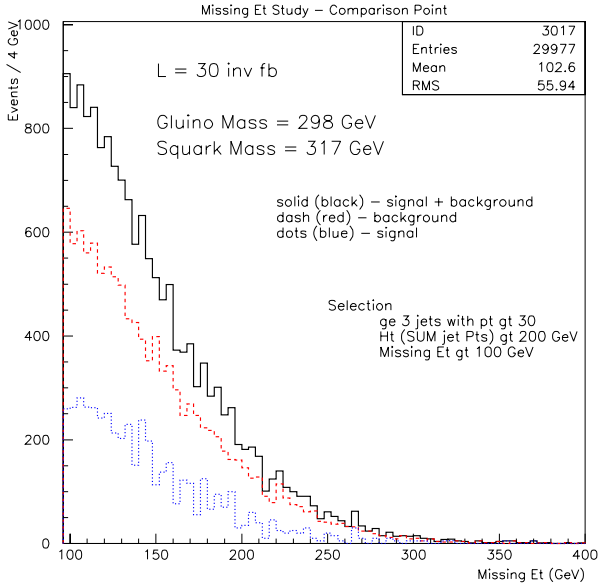

Figure 12: Missing E_T distributions for a 30 fb^{-1} data set selecting events with jets and large H_T.

The SUSY signal for this point is sufficiently large that the excess would be 10 standard deviations with 2 fb^{-1} and a background five times larger than that shown. Previous studies[2] have shown that the reach for the case where $m_{\tilde{g}} \sim m_{\tilde{q}}$ is at least 450 GeV/c^2 for a 30 fb^{-1} run at $\sqrt{s}$ = 2 TeV. If $m_{\tilde{q}} \gg m_{\tilde{g}}$, the gluino mass reach will be $\sim$ 350 GeV/c^2. Thus, discovery via the missing E_T plus jets signature is a serious possibility. Although time did not permit a study, it may also be possible to extract information on the masses and squark-gluino mixture based on the number of jets and p_T distributions.

E. Note on Dilepton Signature

Dileptons will be an important SUSY signature at TeV33. Neutralinos should be copiously produced both in combination with charginos or other neutralinos and in the decays of squarks and gluinos. As shown elsewhere in this report, the dilepton mass spectrum has an edge determined by the mass of the lightest neutralino (for decays not mediated by real sleptons). This edge is useful both for discovery and for determination of the mass difference between the lightest and next-to-lightest neutralino.

In the Comparison Point, the dilepton signal is apparent in association with: 1) b-tags from $\tilde{b}$ decays; 2) trileptons from chargino-neutralino production; and 3) in association with high energy jets. Figure 13 shows the mass distribution for these different cases. In association with high p_T jets, the dilepton mass distribution is shown for a selection of 3 jets ($p_T > 30$ GeV/c) and $H_T > 200$ GeV, both with and without the additional cut of missing $E_T > 100$ GeV. This figure illustrates a variety of measurements of the same quantity from different SUSY production mechanisms. The relative magnitudes of the different distributions are sensitive to the specific SUSY model being considered.

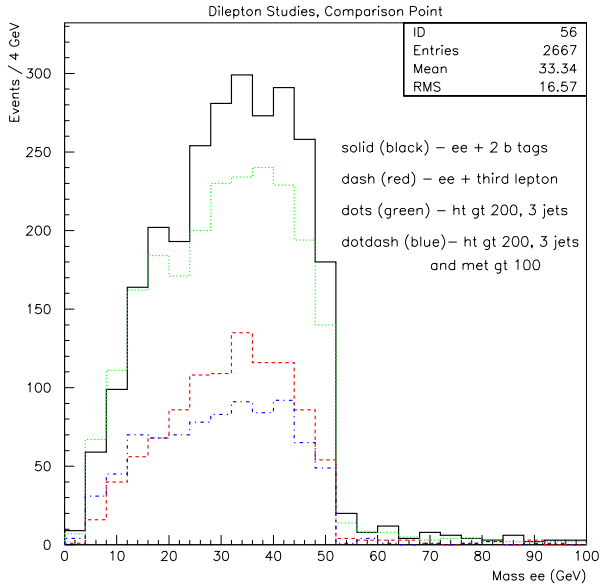

Figure 13: Dilepton mass spectrum from various SUSY processes in the Comparison Point. The edge comes from the decay of the second neutralino which is produced copiously both in association with other neutralinos/charginos and in association with or in the decay of squarks and the gluino.

F. The Light SUSY Top Quark Signature

We investigate the possibility of detecting supersymmetric top squarks via their decays to charged leptons at the Tevatron in Run II and TeV33. For the choice of mSUGRA parameters used as inputs to ISAJET (Point 4), the following facts serve to delineate the analysis strategy:

- The combined masses of the lightest top squark ($m_{\tilde{t}_1} = 140$ GeV/c^2) and the lightest neutralino ($m_{\chi_1^0} = 46$ GeV/c^2) rule out the possibility of a 175 GeV/c^2 SM top decay $t \to \tilde{t}_1 \chi_1^0$.
- The Run I search for stop by the DØ collaboration[14] focused on that part of parameter space for which $m_{\chi_1^\pm} + m_b$, $M_W + m_{\chi_1^0} + m_b > m_{\tilde{t}_1} > m_{\chi_1^0} + m_c$, such that the decay $\tilde{t}_1 \to c\chi_1^0$ dominates. However, for the parameters chosen for this analysis, $m_{\chi_1^\pm} + m_b < m_{\tilde{t}_1}$. In this scenario the decay $\tilde{t}_1 \to b\chi_1^\pm$ is preferred.

The lightest chargino $\chi_1^\pm$ decays to leptons and jets with approximately the same branching fractions as the SM W boson. Because the $\chi_1^\pm$ decay is a three-body decay involving a relatively massive χ_1^0, the p_T spectra of the leptons are soft compared to those from SM top decays. This signature can be exploited to distinguish stop decays from the SM top background.

1. Details of the Stop Analysis

ISAJET v7.20 was used to generate 1000 stop signal events and approximately 2900 SM top events to serve as a background sample. These numbers were chosen to equalize the integrated luminosity for the samples. In both cases decays to dielectron final states were forced. The respective cross sections were 2.2 pb and 6.6 pb for the SUSY signal and top background. The following cuts were applied to the electrons and jets in the events:

- JETS:
  - distinct from EM objects
  - $|\eta^{\rm jet}| < 2.5$
- ELECTRONS:
  - $|\eta^{\rm elec}| < 2.4$
  - Less than 2 Gev of energy in an isolation cone of radius $R = \sqrt{\Delta\eta^2 + \Delta\phi^2} = 0.4$

Shown in Fig. 14 are the p_T spectra for electrons satisfying the cuts just described. The difference in the spectra as previously noted is obvious.

Next, the events were required to have at least two jets with $p_T > 15$ GeV/c, at least two electrons with $p_T > 10$ GeV/c, and $\not\!\!E_T > 20$ GeV. These cuts are similar to those used in Run I top analyses, except for the slightly lower p_T threshold on the electrons necessitated by the softer leptons in stop decays. At this stage 355 stop events and 1960 top events remained in each sample, respectively. This corresponds to a signal-to-background ratio of approximately 1 : 5.5.

To gain better rejection against the top background, two additional cuts were imposed. The quantity H_T, defined as $\sum p_T^{\rm jet\ i} + p_T^{\rm elec\ 1}$, was an effective cut in Run I top analyses for selecting top events and for suppressing vector boson backgrounds (W, Z and WW). For our purposes we required a maximum H_T value to reject the top events.

The second cut was based on a quantity defined as $B = |p_T^{\rm elec\ 1}| + |p_T^{\rm elec\ 2}| + |\not\!\!E_T|$. The softer lepton p_T spectra for stop events make this cut particularly useful against the SM top

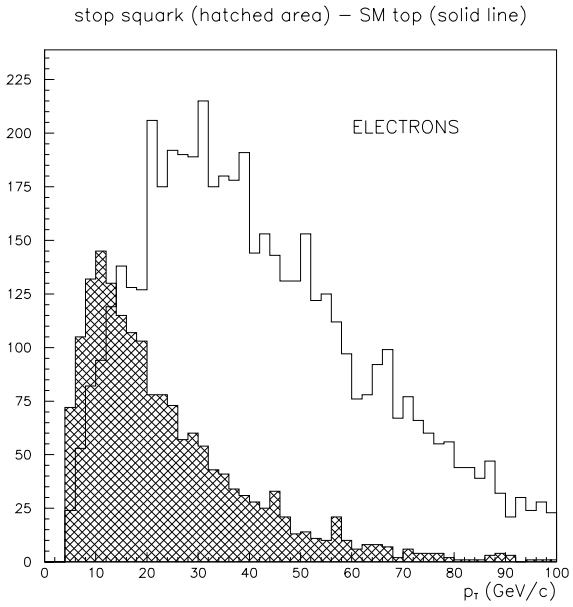

Figure 14: Electron p_T distributions for SUSY signal from Point 4 (hatched) and from top background (clear).

background [15]. In addition, the increased vector boson backgrounds after the H_T cut are reduced as well. We required:

$$B < 100 \text{ GeV}, H_T < 250 \text{ GeV}.$$

Shown in Fig. 15 are the B and H_T distributions for signal and background events passing the cuts imposed on jets, electrons, and $\not\!\!E_T$.

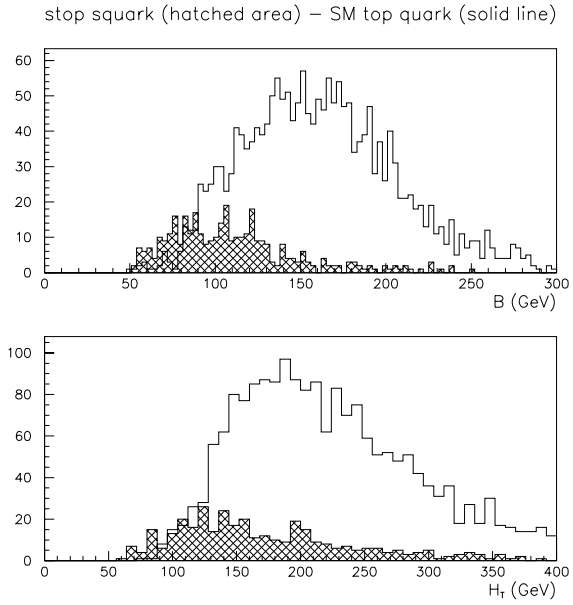

Figure 15: Distributions of the quantities B and H_T (defined in the text) for Point 4 (hatched) and top background (clear) events.

2. Stop Results

After the cuts on B and H_T were applied, 142 and 118 events remained in the stop and top samples respectively, demonstrating the considerable rejection against the SM top background afforded by the cuts. The signal-to-background ratio is now a more favorable 1.2 : 1. Shown in Fig. 16 are the final $\not\!\!E_T$ distributions for the signal and background after all cuts.

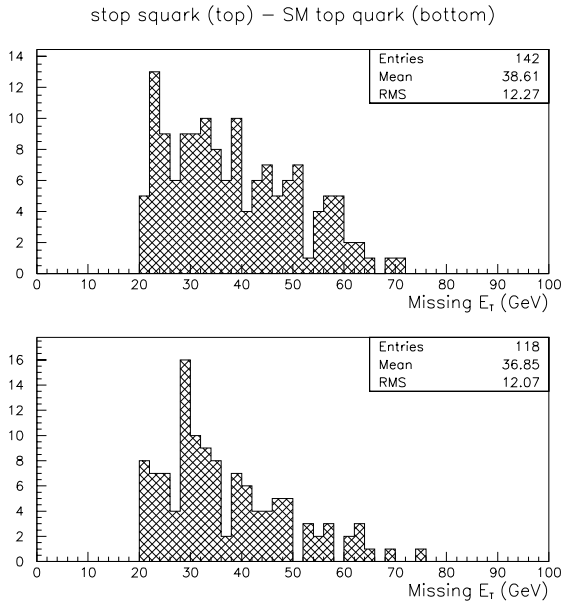

Figure 16: $\not\!\!E_T$ distributions for signal (above) and background (below) events after all cuts.

The results presented here indicate that a supersymmetric stop squark signal can be detected in Run II while reasonably suppressing the background from SM top quark production. The number of expected signal and top background events (142 vs. 118) correspond to slightly less than 37 fb^{-1} of integrated luminosity. With further optimization of cuts it should be possible to improve upon these preliminary numbers.

A few points should be mentioned. A complete detector simulation will likely reduce the overall detection efficiencies by (at least) a factor of 2. This would result in 71 stop events and 59 top events. Other backgrounds not addressed in this discussion (*e.g.*, Z and Drell-Yan $\rightarrow ee$, fake backgrounds in which jets are misidentified as leptons) can be greatly reduced by requiring that both b-jets from the $\chi_1^{\pm}$ (and W) decays are tagged. Assuming a tagging efficiency of 60–70% per b-jet, this yields a combined efficiency of approximately 40%. In this scenario the expected number of stop and top events is 28 vs. 24, respectively for 37 fb^{-1}. Such statistics point out the necessity of a large data sample ($\int \mathcal{L}dt > 20$ fb^{-1}) in Run II to ensure an unambiguous signal in this channel.

Finally we point out that the other dilepton channels ($e\mu$ and $\mu\mu$) are available to increase the statistics of the signal sample. In analogy to the SM top analyses, the lepton + jets channels can yield a measurement of the top squark mass as well as confirm a signal in the dilepton channels. A determination of the stop cross section can be combined with other anticipated SUSY signals to constrain the parameters in the model.

VI. CONCLUSIONS

Previous studies have shown that large regions of supersymmetric parameter space become accessible through a high luminosity program at the Tevatron. At Snowmass, we studied the potential for measuring supersymmetric parameters at a high luminosity Tevatron following discovery for specific SUSY models. The prospects for exploration and measurement at the Tevatron appear to be very promising. A careful consideration of the comparison point shows that many different channels will be accessible and multiple measurements can be made. Based on our studies, we recommend that Fermilab should make a coherent effort to deliver an integrated luminosity of order 25-30 fb^{-1} with reasonably upgraded CDF and D0 detectors, so that new physics searches and measurements may be carried out until the LHC turns on. It should be noted that a light Higgs search may be possible at TeV33; this would be an important concomitant search, since SUSY predicts it to be lighter than 150 GeV/c^2.

VII. REFERENCES

[1] For theoretical motivation and overview, see J. Amundson *et. al.*, *Report of the Supersymmetry Theory Subgroup*, these proceedings, hep-ph/9609374 (1996).

[2] See *Supersymmetric Physics*, in The TeV2000 Group Report, ed. by D. Amedei and R. Brock, Fermilab-Pub-96/082 (1996).

[3] See *e.g.* M. Drees and M. Nojiri, Phys. Rev. **D47**, 376 (1993) and H. Baer and M. Brhlik, Phys. Rev. **D53**, 597 (1996) and references therein.

[4] G.W. Anderson and D.J. Castaño, Phys. Rev. **D52**, 1693 (1995) and Phys. Rev. **D53**, 2403 (1996).

[5] H. Baer, C. Kao, and X. Tata, Phys. Rev. **D48**, R2978 (1993) and Phys. Rev. **D51**, 2180 (1995).

[6] H. Baer, K. Hagiwara and X. Tata, Phys. Rev. **D35**, 1598 (1987); P. Nath and R. Arnowitt, Mod. Phys. Lett. **A2**, 331 (1987); R. Barbieri, F. Caravaglios, M. Frigeni and M. Mangano, Nucl. Phys. B **367**, 28 (1991); H. Baer and X. Tata, Phys. Rev. D **47**, 2739 (1992); J.L. Lopez, D.V. Nanopoulos, X. Wang and A. Zichichi, Phys. Rev. D **48**, 2062 (1993); H. Baer, C. Kao, and X. Tata, Phys. Rev. D **48**, 5175 (1993).

[7] H. Baer, C. Chen, C. Kao and X. Tata, Phys. Rev. **D52**, 1565 (1995) and H. Baer, C. H. Chen, F. Paige and X. Tata, Phys. rev. **D54**, 5866 (1996).

[8] S. Mrenna, G.L. Kane, G.D. Kribs, and J.D. Wells, Phys. Rev. **D53**, 1168 (1996).

[9] LEP experiments announced new results at $\sqrt{s}$ = 140 GeV on December 12, 1995. The new limit on $\tilde{\chi}_1^{\pm}$ is about 65 GeV/c^2.

[10] F. Paige and S. Protopopescu, in Supercollider Physics, p. 41, ed. D. Soper (World Scientific, 1986); H. Baer, F. Paige, S. Protopopescu and X. Tata, in Proceedings of the Workshop on Physics at Current Accelerators and Supercolliders, ed. J. Hewett, A. White and D. Zeppenfeld, (Argonne National Laboratory, 1993), hep-ph/9305342.

[11] See F. Paige, 'Determining SUSY Particles Masses at LHC', these Proceedings.

[12] H. Baer, C. H. Chen, F. Paige and X. Tata, Phys. Rev. **D50**, 4508 (1994).

[13] W.-M. Yao, in 'Measurement of the Gluino-Sbottom Mass Splitting', these Proceedings.

[14] DØ Collaboration, S. Abachi *et al.*, Phys. Rev. Lett. **76**, 2222 (1996).

[15] For stop detection at Tevatron, see H. Baer, M. Drees, R. Godbole, J. Gunion and X. Tata, Phys. Rev. **D44**, 725 (1991) and H. Baer, J. Sender and X. Tata, Phys. Rev. **D50**, 4517 (1994).